CSIRO PUBLISHING

Environ. Chem. **2012**, *9*, 148–157
http://dx.doi.org/10.1071/EN11119

Research Paper

Adsorption of perfluorooctanoic acid and perfluorooctanesulfonic acid to iron oxide surfaces as studied by flow-through ATR-FTIR spectroscopy

Xiaodong Gao[A,B] *and Jon Chorover*[A,C]

[A]Department of Soil, Water and Environmental Science, University of Arizona, Tucson, AZ 85721, USA.
[B]Present address: Department of Earth Science, Rice University, Houston, TX 77251, USA. Email: xdgao@rice.edu
[C]Corresponding author. Email: chorover@cals.arizona.edu

Environmental context. Perfluoroalkyl compounds are organic contaminants that exhibit strong resistance to chemical- and microbial-degradation. As partitioning between solid and aqueous phases is expected to control the transport of perfluoroalkyl compounds, we studied the molecular mechanisms of their adsorption–desorption at a representative Fe oxide surface using in situ molecular spectroscopy. The results provide valuable information on the types of bonds formed, and enable a better understanding of the transport and fate of these organic contaminants in natural environments.

Abstract. The kinetics and mechanisms of perfluorooctanoic acid (PFOA) and perfluorooctanesulfonic acid (PFOS) adsorption to nanoparticulate hematite (α-Fe_2O_3) from aqueous solutions were examined using in situ, flow-through attenuated total reflection Fourier-transform infrared (ATR-FTIR) spectroscopy. Results indicate that both PFOA and PFOS molecules are retained at the hydrophilic hematite surface and the adsorption shows strong pH dependence. However, ATR-FTIR data reveal that PFOA and PFOS are bound to the iron oxide by different mechanisms. Specifically, in addition to electrostatic interactions, PFOA forms inner-sphere Fe–carboxylate complexes by ligand exchange, whereas the PFOS sulfonate group forms outer-sphere complexes and possibly hydrogen-bonds at the mineral surface. Both solution pH and surface loading affect adsorption kinetics. Faster adsorption was observed at low pH and high initial PFC concentrations. Sorption kinetics for both compounds can be described by a pseudo-second-order rate law at low pH (pH 3.0 and 4.5) and a pseudo-first-order rate law at high pH (pH 6.0). Sorption isotherm data for PFOA derived from spectroscopic results exhibit features characteristic of ionic surfactant adsorption to hydrophilic charged solid surfaces.

Received 29 September 2011, accepted 15 February 2012, published online 30 April 2012

Introduction

Perfluoroalkyl compounds (PFCs) such as perfluorooctanoic acid (PFOA) and perfluorooctanesulfonic acid (PFOS) (Fig. 1) are surfactants that have been used as fire extinguishing agents in aqueous film forming foam (AFFF) for decades.[1] AFFF products usually comprise 1–5 % w/w PFCs, including PFOS, PFOA and their short-chain homologues.[2] The unique chemical and thermal stabilities of PFCs are the principal reasons for their use in AFFFs.[3] The physicochemical properties of PFCs differ significantly from their hydrocarbon analogues. Substitution of H by electronegative F in the aliphatic chain structure gives rise to very high C–F bond covalency. Relative to their hydrocarbon analogues, fluorination increases the rigidity of the carbon chains, compound thermal stability and Brønsted acidity of the acid group (Table 1).[4–7]

Historically, effluents from AFFF fire-fighting activities were not pre-treated before discharge to waste-water treatment systems or to the environment, and military activities are an important contributor. For example, because of the use of large quantities of flammable liquids, the USA military consumes ~75 % of total nationwide AFFF production each year, resulting in numerous PFC contaminated sites within the Department of Defence complex that require cleanup.[3,8] It is estimated that a total of 50–100 t of PFOA and 3–30 t of PFOS have been released to the environment from historical use of AFFF products in the USA.[1] PFCs can cause developmental toxicity, immunotoxicity, hepatotoxicity and hormonal effects even at very low concentrations.[9,10] Thus, it is essential to establish a mechanistic understanding of the geochemical processes that govern the transport and fate of PFCs in soil and water systems, and that can be used in remediation technologies for effective contaminant removal.

The global occurrence and distribution of PFCs has only recently become a focus of study. Despite the fact that PFCs have been widely identified in surface water,[11–13] groundwater,[8,13] public drinking water systems[14,15] and sea water,[11,16] little is known about their transport and fate in the environment. Because of their remarkable resistance to chemical- and microbial-degradation in geomedia,[17] sorption–desorption dynamics are expected to be a key control on environmental fate. Upon release to soils and sediments, the reactive transport of PFCs in terrestrial systems is governed largely by surface interactions with soil and sediment particles. A recent soil column study reported that PFOS in street runoff

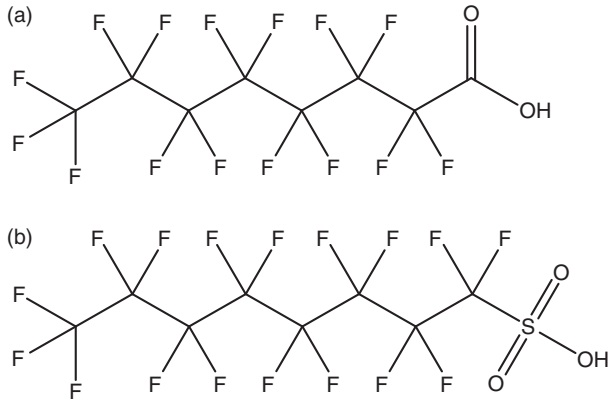

Fig. 1. Chemical structure of (a) perfluorooctanoic acid (PFOA, $C_7F_{15}COOH$) and (b) perfluorooctanesulfonic acid (PFOS, $C_8F_{17}SO_3H$).

Table 1. Physico-chemical properties of the perfluoroalkyl compounds (PFCs) perfluorooctanoic acid (PFOA) and perfluorooctanesulfonic acid (PFOS)[4–7]

CMC, critical micelle concentration

PFCs	Molecular formula	Water solubility ($mg\,L^{-1}$)	pK_a	CMC (mM)	log K_{ow}
PFOA	$CF_3(CF_2)_6COO^-$	3400	2.6	8.7–9.0	4.3
PFOS	$CF_3(CF_2)_7SO_3^-$	570	<1	2.0	5.3

was not removed during the infiltration process and in fact the concentration of PFOS was observed to increase along the flow path, which was attributed to its formation from precursor compounds.[13] This study and several other recent reports[12,18] suggest that PFCs can be relatively mobile in the subsurface and may cause groundwater contamination. PFCs are strong acids that dissociate to anionic form in most natural environments. Thus, anionic PFCs are expected to adsorb to positively charged surfaces (e.g. Al and Fe oxides) by electrostatic or covalent bonding interactions. In addition, because of its unique composition, the fluorocarbon tail exhibits both hydrophobic and lipophobic properties, and fluorocarbon chain length controls the extent to which the compound undergoes intermolecular aggregation and adsorbs to hydrophobic surfaces such as natural organic matter (NOM).[19]

The energetics of surfactant adsorption result from the additive effects of multiple bonding modes, including the Gibbs energies of molecular and surface hydration, and intermolecular associations. In general, molecular mechanisms of adsorption can include covalent (inner-sphere) or electrostatic (outer-sphere) complexation at surface sites, hydrophobic interaction (including intermolecular associations such as surface admicelle and hemimicelle formation), ion or water bridging and hydrogen bonding.[20] Prior macroscopic studies indicate that adsorption of PFCs is strongly influenced by aqueous geochemistry and sorbent properties. Adsorption of PFCs to several natural sediments, clays, synthetic iron oxide (goethite, no organic carbon) and activated carbon shows positive correlation with organic matter content[21,22] and compound fluorocarbon chain length,[21,23] indicating that PFC hydrophobicity contributes to sorption energetics. Adsorption of PFCs to sediments also increases with decreasing pH and charge fraction of bivalent cation (Ca^{2+}),[21,22,24,25] suggesting that electrostatic interaction of the polar anionic PFC head with charged solids and bridging cations plays an important role in adsorption. Sorption mechanisms, however, cannot be unambiguously determined from these macroscopic experiments. Molecular-scale adsorption mechanisms of PFCs at solid surfaces remain largely unexplored. In addition, PFCs can potentially form surface-induced hemimicelles at solid–water interfaces well below the critical micelle concentration (CMC) (0.1–1.0 % of the CMC).[22] As a result, the adsorption mechanisms of PFCs are likely to vary significantly across the environmentally relevant concentration range. Studies are clearly needed to develop a comprehensive understanding of molecular-scale sorption processes as affected by geochemical conditions as they control the transport and fate of PFCs in natural soil and water systems.

Attenuated total reflection Fourier-transform infrared (ATR-FTIR) spectroscopy is an established in situ technique for interrogating molecular sorption mechanisms, redox processes and reaction kinetics in aqueous systems.[26–29] Recently, ATR-FTIR has been increasingly applied to the determination of adsorption kinetics and detailed molecular-level information of the coordination and structure of various adsorbates at the solid–water interfaces, including inorganic anions (e.g. sulfate, phosphate and arsenate),[30,31] low-molecular-weight (LMW) carboxylic acids,[32] extracellular polymeric substance (EPS) and intact microbial cells[28,33] and hydrocarbon ionic surfactants.[29,34,35] To our knowledge, however, there are no prior ATR-FTIR studies of adsorption of PFCs from aqueous solution onto environmental solid surfaces. The primary objective of this study, therefore, was to examine the binding mechanisms and kinetics of PFOA and PFOS, the two most common components of PFCs in AFFF products, onto the surface of a representative Fe^{III} oxide (hematite, α-Fe_2O_3) across a gradient in pH that is characteristic of natural pore waters present in soils and sediments. Hematite was chosen as the model surface because it is one of the most abundant Fe (oxyhydr)oxides in highly weathered soils or sediments, and it often occurs naturally in nanoparticulate, high specific surface area forms, which can serve as a high affinity sorbent for PFCs.[36] ATR-FTIR spectroscopy was employed in conjunction with a flow cell technique to elucidate in situ dynamic changes in spectroscopic data of PFOA and PFOS as affected by solution chemistry and binding to solid surfaces.

Experimental methods

Chemicals and materials

PFOA (96 %) and PFOS as the potassium salt (>98 %) were purchased from Sigma–Aldrich Co. (St Louis, MO) and used as received. Synthesis of nanoparticulate α-Fe_2O_3 was performed following the methods of Schwertmann and Cornell.[36] The detailed synthetic procedure and characterisation have been given previously.[28] The synthetic hematite has a particle size of ~10–20 nm in diameter, a Brunauer–Emmett–Teller (BET) N_2 specific surface area of $69.3 \pm 0.3\,m^2\,g^{-1}$, and a measured isoelectric point (IEP) of ~7.7–7.8 in 1 mM $NaNO_3$ background electrolyte.[28,29] All solutions were prepared using Barnstead Nanopure (BNP) water (Thermal Scientific, Waltham, MA; 18.2 MΩ cm) in a background electrolyte solution containing 10 mM NaCl (except for the ionic strength study) with pH adjustment by addition of NaOH or HCl.

FTIR spectroscopy measurements

ATR-FTIR spectra were obtained with a Magna-IR 560 Nicolet spectrometer (Madison, WI) equipped with a purge gas generator and a deuterated triglycine sulfate (DTGS) detector.

A 45° trapezoidal germanium internal reflection element (IRE) ($56 \times 10 \times 3$ mm^3) in a flow-through cell (Pike Technologies, Madison, WI) was employed. The Ge IRE in the flow cell was coated with ~1.65 mg nanoparticulate hematite as described by Gao et al.[28] and placed on a horizontal ATR sample stage inside the IR spectrometer. The thickness of the hematite coating was calculated to be ~0.6 μm. A new coating was prepared for each experiment, and spectra of dry films were collected to determine the consistency of the coating. The cell was connected to a reaction vessel containing 1 L of background electrolyte solution, with and without PFCs, continuously stirred with a magnetic bar. A peristaltic pump was used to deliver the background electrolyte or PFC solutions from the reaction vessel through the flow cell at a constant flow rate of 0.5 mL min^{-1}. The effluent from the flow cell was collected to waste.

All spectra were acquired at 4.0 cm^{-1} resolution with 400 scans over the spectroscopic range of 4000–800 cm^{-1} using the autogain function and aperture set at 100 at room temperature. For each experiment, background electrolyte solution (10 mM NaCl) was first pumped through the cell, allowing the hematite coating to equilibrate with the background solution. Successive background spectra of 10 mM NaCl at the hematite-coated Ge IRE were collected during the equilibrium time under continuous flow conditions. The final background spectrum was collected when no further changes in the spectra were observed and this background was used for the remainder of the experiment. PFOA or PFOS in 10 mM NaCl electrolyte solution was then injected into the cell to initiate the adsorption experiment. Spectra were collected as a function of pH (3.0–6.0) and compound concentration (50–1000 μM for PFOA and 50–250 μM for PFOS). Experiments were also conducted at pH 9.0, which is higher than the point of zero net proton charge (pH_{pznpc}) of hematite (pH 7.7–7.8), but spectroscopic intensities were observed to decrease with increasing pH and became undetectable by FTIR at pH 9.0. PFOS adsorption was examined over a lower concentration range due to its lower water solubility and CMC (Table 1). The pH of the solution in the reaction vessel was monitored throughout the experiments, and adjusted as necessary by addition of 10 mM NaOH or HCl. Adsorption kinetics of PFOA or PFOS on hematite were monitored by collecting spectra at 15 min intervals until adsorption equilibrium was attained as indicated by no further changes between successive spectra. Following the adsorption experiment, PFC-free background electrolyte solution was introduced again to the ATR cell to assess desorption kinetics. Spectra were collected every 15 min until no change was observed in subsequent spectroscopic data over a time scale of <120 min and this was defined as the apparent desorption equilibrium. The effect of ionic strength on PFOA adsorption was also examined in a separate experiment in 1, 10 and 100 mM NaCl background electrolyte using the same method described above.

All spectra (adsorption and desorption) were obtained by subtracting the final background spectrum of hematite in the corresponding NaCl background electrolyte. Data collection and spectroscopic processing, including background subtraction and baseline correction, were performed using the OMNIC program (Thermo Nicolet, Co., Madison, WI). The GRAMS/AI software (Thermo Electron Corp., Madison, WI) was used for peak deconvolution and to determine the position and area of the IR bands. A linear baseline was applied to the raw spectra. The baseline corrected spectra were then fitted with Lorentzian peaks. No constraints were placed on any of the fitting parameters (e.g. peak position, width or intensity).

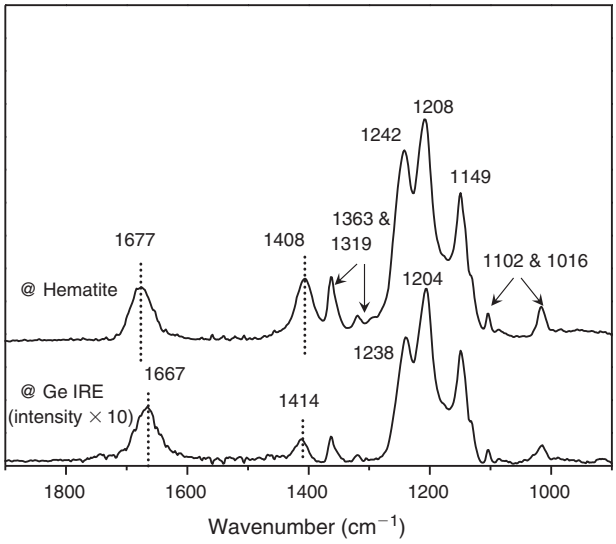

Fig. 2. Attenuated total reflection Fourier-transform infrared spectra of 500-μM perfluorooctanoic acid adsorbed on Ge internal reflection element (IRE) and hematite surface in 10 mM NaCl solution at pH 6.0. The absorbance intensity of the spectrum at Ge IRE was increased 10 times for comparison.

Results and discussion

FTIR spectra of dissolved and hematite-adsorbed PFOA

The ATR-FTIR spectrum of aqueous PFOA on the Ge IRE in the absence of nanohematite coatings represents that of the dissolved species. Adsorption to the Ge IRE is expected to be negligible because of electrostatic repulsion between the negatively charged Ge IRE and the anionic surfactant. The spectrum is dominated by strong asymmetric and symmetric stretching bands of the CF_2 and CF_3 groups of the hydrophobic tail and the deprotonated carboxylate head groups (COO^-) (Fig. 2). Detailed peak position and mode assignments are given in Table 2.[26,28,37,38] As PFOA, a monocarboxylic acid with relatively high acid strength ($pK_a = 1.31$–2.8 depending on experimental conditions),[39,40] is nearly fully deprotonated throughout the pH range probed by this study (≥pH 3.0), the carboxylate stretching bands in aqueous form are not expected to exhibit systematic changes with solution pH.

In the presence of the hematite coating, absorbance intensities in the PFOA spectrum are much greater (~10-fold higher) than those for the aqueous form (Fig. 2). The positive effect of hematite on PFOA adsorption can be attributed to favourable electrostatic interactions between the positive-charged hematite surface ($pH_{pznpc} = 7.7$–7.8)[28] and the anionic surfactant, in addition to an increase in total surface area of the solid–water interface probed by the IR beam when nanoparticulate hematite is present.[29] The spectrum of hematite-adsorbed PFOA is very similar to its aqueous form, exhibiting major bands corresponding to the stretching bands of COO^-, CF_2 and CF_3 groups.

Despite overall similarities between the two spectra (Fig. 2), close examination reveals that significant changes in the carboxylate stretching region results from the presence of hematite, indicating that the negatively charged COO^- groups play a role in interfacial reaction. For example, compared with the aqueous PFOA spectrum, the peak position of $\nu_{as}(COO^-)$ in the presence of hematite is shifted to a higher wavenumber, from 1667 to 1677 cm^{-1}, whereas the $\nu_s(COO^-)$ is shifted to a slightly lower wavenumber (from 1414 to 1408 cm^{-1}), resulting in an increase

Table 2. Positions (cm^{-1}) and mode assignments of major IR bands in attenuated total reflection Fourier-transform infrared spectra of aqueous perfluorooctanoic acid (PFOA) and perfluorooctanesulfonic acid (PFOS) (pH 6.0) on the Ge internal reflection element

ν_{as}, asymmetric stretch; ν_s, symmetric stretch; ν_{ax}, axial stretch

PFOA		PFOS	
Wavenumber (cm^{-1})	Mode assignment	Wavenumber (cm^{-1})	Mode assignment
1667	$\nu_{as}(COO^-)$	1372	$\nu_{ax}(CF_2)$
1414	$\nu_s(COO^-)$	1329	$\nu_{ax}(CF_2)$
1363	$\nu_{ax}(CF_2)$	1283	$\nu(CF_2)$
1319	$\nu_{ax}(CF_2)$	1267	$\nu(CF_2)$
1238	$\nu_{as}(CF_2)$	1243	$\nu_{as}(CF_2) + \nu_{as}(R–SO_3^-)$
1204	$\nu_{as}(CF_2) + \nu_{as}(CF_3)$	1215	$\nu_{as}(R–SO_3^-)$
1149	$\nu_s(CF_2)$	1152	$\nu_s(CF_2)$
1102	ν(C–C)	1066	$\nu_s(R–SO_3^-)$
1014	ν(C–C)	1037	ν(C–C)

in separation ($\Delta\tilde{\nu}$) between these two stretching bands. Similar shifts in the ν_{as} and ν_s peak positions have been previously observed for LMW carboxylic acid (L-lactate) adsorbed on hematite nanoparticles.[41] These shifts were attributed to the formation of inner-sphere complexes between lactate carboxylate groups and hematite surface Fe atoms. In addition, the intensity ratio of ν_s to ν_{as} for COO^- stretching increased upon PFOA adsorption to hematite (Fig. 2). Prior studies indicate that increased values of the $\nu_s(COO^-)$ to $\nu_{as}(COO^-)$ intensity ratio upon adsorption are a diagnostic feature of inner-sphere complexation with mineral surface metal centres.[28,32,42] Thus, the results suggest that the carboxylate head groups of PFOA form inner-sphere (i.e. covalent) bonds at the hematite surface. The asymmetric stretching bands of CF_2 groups were also shifted slightly to higher wavenumbers, apparently because of local changes in the PFOA molecular environment encountered at the solid–water interface upon adsorption (Fig. 2).

Although ATR-FTIR data clearly indicate that PFOA is adsorbed to hematite by inner-sphere complexes, the additional contribution of outer-sphere complexes cannot be excluded under the experimental conditions, as the hematite surface and surfactant molecules are oppositely charged. Variation in ionic strength is often used as an indirect test of the contribution of inner- and outer-sphere complex modes of metal or anion adsorption to charged surfaces.[43] If inner-sphere complexation is the sole sorption mechanism, adsorption should not be significantly affected by a change in the ionic strength of 'indifferent' (non-surface complexing, e.g. NaCl) background electrolyte, whereas if outer-sphere complexation is a predominant sorption mechanism, the extent of adsorption should decrease with increasing ionic strength. In the present study, PFOA adsorption to hematite was measured as a function of ionic strength (NaCl as background electrolyte) at three different pH values (3.0, 4.5 and 6.0). The adsorption, as represented by the absorbance of the $\nu_{as}(CF_2)$ band centred at 1208 cm^{-1}, decreases with increasing ionic strength at all pH values, indicating that, in addition to ligand exchange reactions, outer-sphere complexation also plays a role in PFOA adsorption (Fig. 3). A negative effect of ionic strength on adsorption was also observed in a batch study of PFOS adsorption on goethite.[25] In the pH range of the present study (3.0–6.0), the electrostatic attractive force between the positively charged hematite surface and negatively charged PFOA molecules was evidently diminished by charge screening or adsorptive competition with the background ions (i.e. Na^+ and Cl^-). Hence,

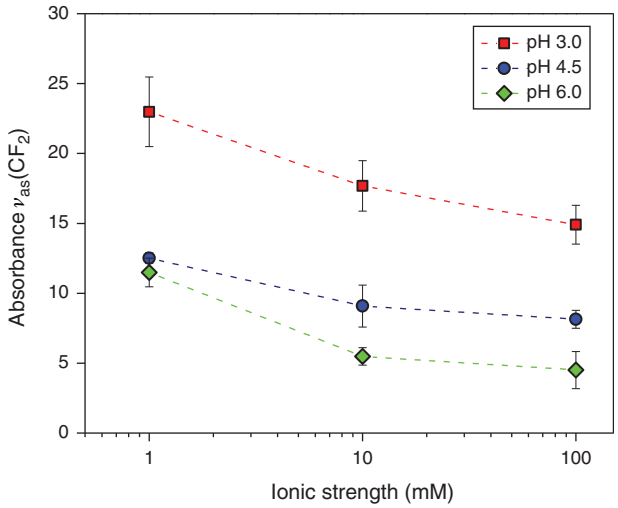

Fig. 3. Effect of ionic strength on perfluorooctanoic acid adsorption on hematite at pH 3.0, 4.5 and 6.0 shown by the absorbance of the $\nu_{as}(CF_2)$ band centred at 1208 cm^{-1}.

although the ATR-FTIR data clearly show a ligand exchange reaction for PFOA at the hematite surface, decreased adsorption with increasing ionic strength suggests that a portion of PFOA may be adsorbed by electrostatic interaction. The fact that a distinct second $\nu_{as}(COO^-)$ peak characteristic of outer-sphere complexation was not observed at a lower wavenumber suggests that both complexed and non-complexed carboxylate vibrational modes may be overlapping to give rise to the broad 1677 cm^{-1} band.

FTIR spectra of dissolved and hematite-adsorbed PFOS

The structure of PFOS is similar to that of PFOA, but with sulfonate replacing carboxylate in the polar head group, along with the addition of a single CF_2 group (Fig. 1). Consequently, PFOS exhibits stronger acidity ($pK_a < 1$) and a lower CMC (2.0 mM) than PFOA.[5,7] Spectra of PFOS at the Ge IRE (dissolved) and hematite surface (adsorbed) are shown in Fig. 4. The two spectra are very similar except for the intensity difference. Similar to PFOA, PFOS exhibits a much higher affinity for the hematite surface as a result of electrostatic attraction and increased interfacial area produced by the hematite film. The peak positions of major sulfonate and CF_2 stretching bands occur with consistent relative intensities and peak locations in

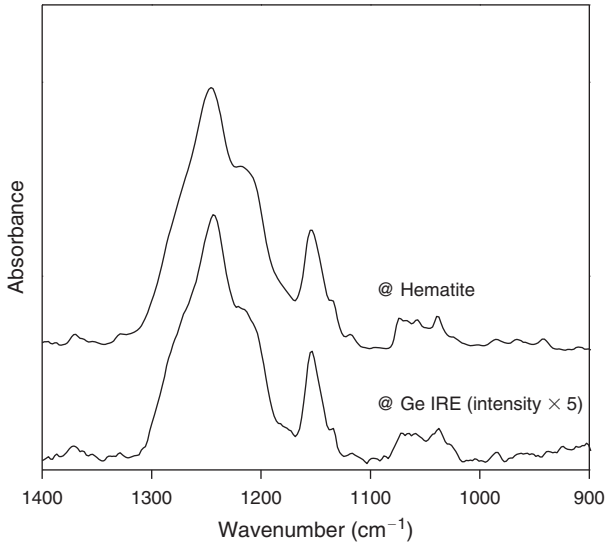

Fig. 4. Attenuated total reflection Fourier-transform infrared spectra of 250-μM perfluorooctanesulfonic acid adsorbed on Ge internal reflection element (IRE) and hematite surface in 10 mM NaCl solution at pH 5.0. The absorbance intensity of the spectrum at Ge IRE was increased five times.

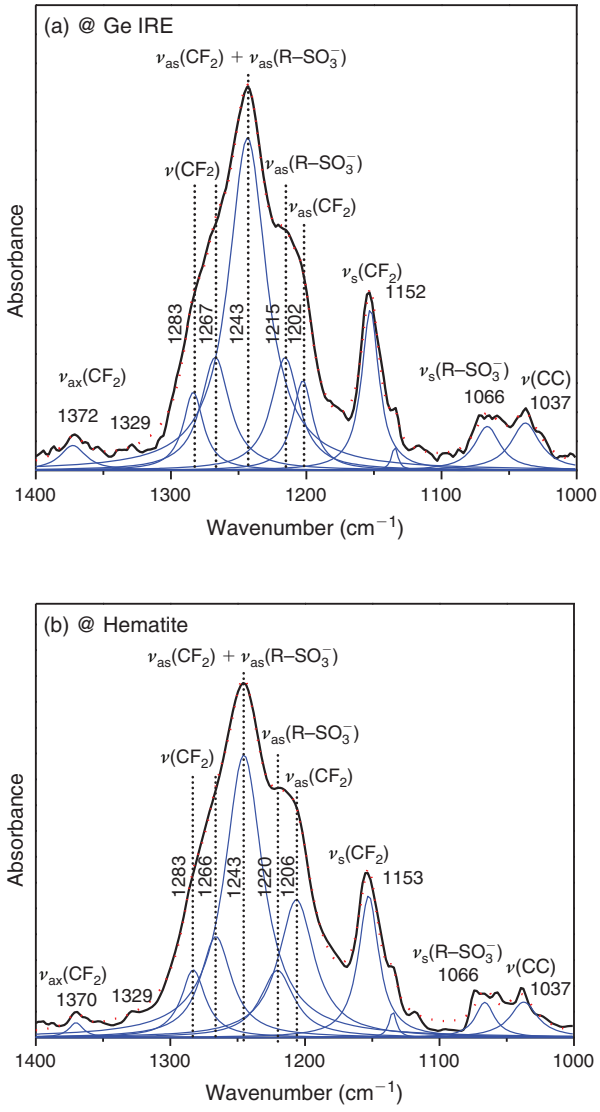

Fig. 5. Peak deconvolution of the perfluorooctanesulfonic acid spectra (250 μM) on (a) Ge internal reflection element (IRE) and (b) hematite in 10 mM NaCl solutions at pH 5.0. The solid line is the experimental data. The red dash line represents the non-linear least square fit. The blue lines are the deconvoluted peaks.

the spectroscopic region 1300–1100 cm^{-1}. Precise assignment of individual IR bands was obtained by peak fitting and deconvolution. As shown in Fig. 5a, the set of bands determined by peak deconvolution is consistent with those previously reported in the literature.[26,29,37,38] The absorption bands at 1283, 1267, 1243 and 1202 cm^{-1} correspond to asymmetric and symmetric CF_2 stretching bands that are also present in the spectrum of PFOA. The additional band at ~1215 cm^{-1} can be assigned to $\nu_{as}(R–SO_3^-)$.[29,34] Sulfonate groups are very sensitive to changes in local coordination geometry. For example, a symmetry change of sulphate and sulfonate groups may result in splits or shifts of the asymmetric vibrations (ν_3).[30,44] The sulfonate group in the PFOS structure has $C_{3\nu}$ symmetry, which is expected to exhibit doublet peaks corresponding to a doubly degenerate band at a higher wavenumber (~1240 cm^{-1}) and a non-degenerate band at a lower wavenumber (~1210 cm^{-1}).[29,34,35] Thus, we attribute the strong band centred at 1243 cm^{-1} to a combination of $\nu_{as}(CF_2)$ and $\nu_{as}(R–SO_3^-)$. This assignment is also supported by the fact that the band became the strongest band in the spectrum whereas the other $\nu_{as}(CF_2)$ band (i.e. 1204 cm^{-1}) is the strongest band in the spectrum of PFOA in the absence of interference from sulfonate stretching. Band assignments are summarised in Table 2.

Peak fitting results of the hematite-adsorbed PFOS spectrum are very similar to those obtained for the aqueous phase species (Fig. 5b). The $\nu_{as}(R–SO_3^-)$ manifests as a doublet corresponding to the $C_{3\nu}$ symmetry, indicating that the symmetry of the sulfonate group was not changed upon adsorption, and therefore, no direct chemical bond formed between the sulfonate groups and hematite surface. Nevertheless, we observed slight spectroscopic changes in the region of asymmetric sulfonate stretching. Compared with the spectrum of aqueous PFOS, one of the $\nu_{as}(R–SO_3^-)$ bands shifted from 1215 to 1220 cm^{-1}, and the intensity of this band was diminished relative to other bands in the spectrum (Fig. 5). Similar changes were observed in a previous study of sodium dodecyl sulfonate (SDS, a hydrocarbon anionic surfactant) adsorption to hematite.[29] The two $\nu_{as}(OSO_3^-)$ bands correspond to a doubly degenerate E vibration and a second non-degenerate A vibration with the directions of the transition dipole moment perpendicular to each other.[29,35] The A vibration at 1220 cm^{-1} is more sensitive to direct contact with charged solid surfaces, whereas the E vibration mode at 1243 cm^{-1} is sensitive to lateral surfactant–surfactant interactions.[35] Thus, the change in the A vibration mode of $\nu_{as}(R–SO_3^-)$ upon adsorption to hematite indicates a change in the local environment of the sulfonate head, possibly attributable to hydrogen-bond formation between the sulfonate group and hematite surface hydroxy groups.[29,34]

Effect of solution pH on PFOA and PFOS adsorption

Several recent ATR-FTIR spectroscopic studies of adsorption of LMW carboxylic acids on various hydroxylated mineral surfaces (e.g. α-Fe_2O_3, Al_2O_3 and TiO_2) indicate that carboxylate groups can form either inner-sphere or outer-sphere complexes at the oxide–water interface, and that solution pH plays an important role in the process.[32,42,45] The effect of pH on PFOA adsorption was, therefore, examined in this study. Adsorption of

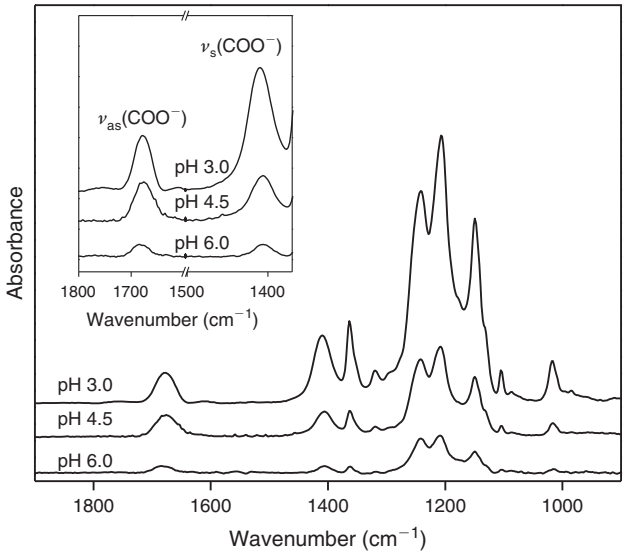

Fig. 6. Attenuated total reflection Fourier-transform infrared spectra of 500-μM perfluorooctanoic acid adsorbed to hematite surface as a function of pH.

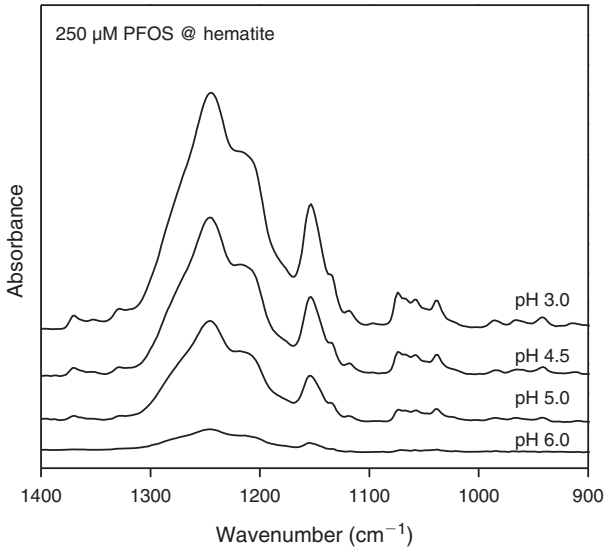

Fig. 7. Attenuated total reflection Fourier-transform infrared spectra of 250-μM perfluorooctanesulfonic acid (PFOS) adsorbed to hematite surface as a function of pH.

PFOA to hematite, as measured by FTIR absorbance intensities, exhibits strong pH dependence (Fig. 6). Adsorption increases substantially with decreasing pH from 6.0 to 3.0 (no detectable IR signals at pH ≥ 7.0 under the flow conditions), consistent with prior macroscopic adsorption studies.[21,25] The stronger adsorption at low pH can be partially attributed to favourable electrostatic forces. At pH < pH_{pznpc} of hematite (7.7–7.8), adsorption is certainly affected by electrostatic attractions between the negatively charged carboxylate and positively charged hematite surface functional groups. Adsorption is negligible at pH > pH_{pznpc} of hematite where, in the presence of an indifferent background electrolyte, PFOA and the hematite surface are both net negatively charged. Despite similarities among the spectra across the pH range, small pH-dependent changes in carboxylate stretching vibrations were observed. The intensity ratio of $\nu_s(COO^-)$ to $\nu_{as}(COO^-)$ increases with decreasing pH (Fig. 6, inset), suggesting that inner-sphere metal–carboxylate complexes are favoured at low pH, similar to what has been previously reported for hematite adsorption of LMW carboxylic acids[32] and carboxylate groups of microbial surface biomacromolecules.[28] Therefore, in addition to electrostatic attraction, ligand exchange of carboxylate groups at mineral surface hydroxy groups also contributes to enhanced adsorption at low pH.

Similar to PFOA, the adsorption of PFOS to hematite also shows strong pH dependence (Fig. 7). Adsorbate surface excess increases with decreasing pH, consistent with prior batch sorption studies.[21,22,25] Other than increased intensity, no detectable changes were observed in the spectroscopic shape across the pH range, indicating that electrostatic attraction is dominantly responsible for the strong pH-dependence of adsorption.

Adsorption kinetics of PFOA and PFOS

Integrated absorbances of IR bands have been used previously to assess surface excess of surfactants at solid surfaces.[26,46] The penetration depth (d_p) of the IR evanescent wave (0.16–1.6 μm for the spectroscopic range of 4000–400 cm^{-1} with the 45° Ge IRE used in this study) may be greater than the layer of interfacial sorption and extend into the bulk solution. Thus, in addition to adsorption at the solid–water interface, the measured IR absorbance may also contain contributions from isotropic bulk solution.[26,46] However, as discussed above, as the absorbance intensities of the aqueous PFOA spectrum are < 1/10 of those for the hematite-adsorbed form, we assume that the contributions from the isotropic bulk media are negligible in this experiment. Therefore, the kinetics of PFOA adsorption to hematite were assessed by directly monitoring the intensity change of its fluorocarbon IR band – specifically the $\nu_{as}(CF_2)$ band centred at 1208 cm^{-1} that does not shift significantly with solution chemistry and surface loading during the flow through experiment. Adsorption was relatively rapid at all pH values, reaching equilibrium within a few hours, but the rate and extent of the adsorption increased significantly with decreasing pH (Fig. 8). At pH 6.0, adsorption increased progressively with reaction time and achieved equilibrium after 6 h. Adsorption at

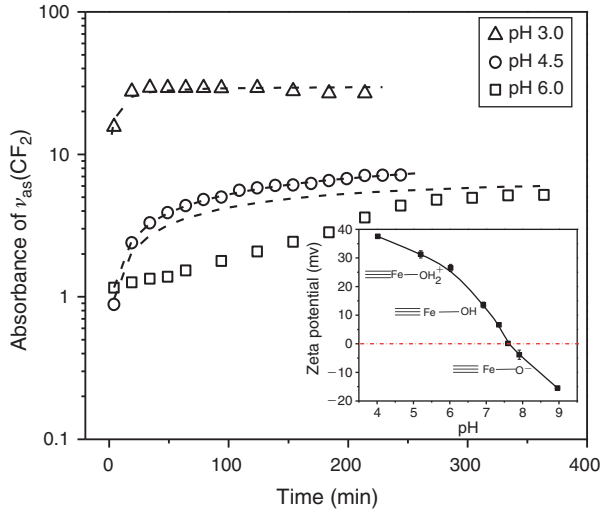

Fig. 8. Adsorption kinetics of 500-μM perfluorooctanoic acid on hematite as represented by the IR absorbance of $\nu_{as}(CF_2)$ band at 1208 cm^{-1}. Fitting results of the pseudo-first-order (pH 6.0) and pseudo-second-order models (pH 4.5 and 3.0) are plotted as dash lines. The inset presents the zeta potential of hematite (0.1 g L^{-1}) as a function of pH in 1 mM $NaNO_3$ solution.

Table 3. Fitting parameters of the pseudo-first-order and pseudo-second-order models for perfluorooctanoic acid (PFOA) adsorption on hematite from 500 µM PFOA aqueous solution at different pH

$q_{e,exp}$, experimental equilibrium sorption uptake as represented by IR absorbance (peak area) of $\nu_{as}(CF_2)$; $q_{e,cal}$, calculated equilibrium sorption uptake

Solution pH	$q_{e,exp}$	Pseudo-first-order			Pseudo-second-order		
		$q_{e,cal}$	k_1 (min^{-1})	R^2	$q_{e,cal,}$	k_2 (min^{-1})	R^2
3.0	29.337	–	–	–	29.851	0.0105	0.9998
4.5	7.150	–	–	–	8.489	0.0022	0.984
6.0	5.190	6.994	0.0092	0.932	7.530	0.0007	0.774

pH 3.0 was much more rapid, reaching an adsorption maximum within 30 min. The difference can be attributed to the pH-dependent surface charge of hematite (Fig. 8, inset). At pH 3.0, hematite surface hydroxy groups that can undergo protonation are in a fully protonated state, giving rise to maximum positive surface charge and, therefore, exhibit high affinity for anionic surfactant molecules. The kinetics of ligand exchange are also expected to be increased under these conditions, where inner-sphere complexation of the PFOA carboxy group is promoted by the dissociation of the water molecule from the Fe^{III} surface metal centre[47]:

$$\equiv Fe - OH_2^+ + CF_3(CF_2)_6COO^- \rightarrow \equiv Fe - OOC(CF_2)_6CF_3 + H_2O \quad (1)$$

Relative to its neutral (≡Fe–OH) or deprotonated forms (≡Fe–O^-), protonation of the hematite surficial hydroxy groups reduces the activation energy for ligand exchange and, thereby increases their substitutional lability.[47] Thus, a large concentration of protonated sites at low pH evidently increases the reaction rate of Eqn 1. With increasing pH, the hematite surface becomes progressively deprotonated, resulting in a decrease in adsorption kinetics and equilibrium extent. The slower second step adsorption kinetics at high pH is consistent with a sorption barrier generated by structural re-arrangement and surfactant self-assembly of adsorbed PFOA at the solid–water interface.[26] In addition, intra- and interparticle diffusion into the porous hematite film may also contribute to the slow kinetics.[48] This observation contrasts with prior studies pertaining to adsorption of hydrocarbon analogues of PFOA and PFOS. Adsorption of hydrocarbon ionic surfactants to charged particles is generally rapid, reaching sorption equilibrium within minutes irrespective of solution pH.[29,45] One possible explanation for this discrepancy is the size and hydrophobicity differences between the two types of compounds. Substitution of H by F in the aliphatic chain structure increases the molecular size and hydrophobicity of PFCs relative to hydrocarbon analogues. This may limit their diffusion in the hydrophilic sorbent film and thereby contribute to the slow sorption kinetics.

Adsorption kinetic data were fit to pseudo-first-order (Eqn 2) and second-order (Eqn 3) models to facilitate interpretation of the rate controlling sorption processes.[48–50]

$$\log(q_e - q_t) = \log q_e - \frac{k_1}{2.303}t \quad (2)$$

$$\frac{t}{q_t} = \frac{1}{k_2 q_e^2} + \frac{t}{q_e} \quad (3)$$

where q_t is the adsorbed mass of PFCs at time t (represented by the absorbance of the $\nu_{as}(CF_2)$ band); q_e is the equilibrium adsorbed mass, and k_1 and k_2 are the first and second-order adsorption rate coefficients. As shown in Fig. 8 and Table 3, adsorption at pH 3.0 is well described by a pseudo-second-order reaction equation with the correlation coefficient $R^2 = 0.9998$ and the calculated sorbate concentration at equilibrium ($q_{e,cal}$) close to the measured value ($q_{e,exp}$). Adsorption at pH 4.5 is also fairly well fit to pseudo-second-order kinetics ($R^2 = 0.984$). However, the $q_{e,cal}$ is much larger than $q_{e,exp}$ in this case, suggesting that adsorption equilibrium may not have been reached during the experimental time frame. As shown in Table 3, adsorption kinetics at pH 6.0 are better described by a pseudo-first-order model (Table 3). However, this model still clearly over-predicts adsorption at early times (<250 min) (Fig. 8). The kinetics of PFOS adsorption to hematite exhibits similar trends (Fig. 9). Increasing pH diminished both the PFOS uptake rate and extent.

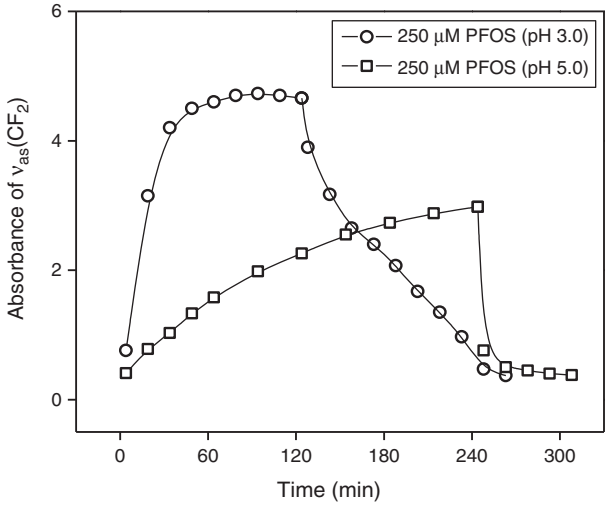

Fig. 9. Adsorption–desorption kinetics of perfluorooctanesulfonic acid (PFOS) on hematite as represented by the IR absorbance of the $\nu_{as}(CF_2)$ at pH 3.0 and 5.0

The concentration of surfactant in the bulk solution significantly affects PFOA adsorption kinetics. As shown in Fig. 10, increasing the initial PFOA concentration from 50 to 1000 µM not only increased the extent of equilibrium uptake, but the adsorption rate coefficient as well. Time to adsorption equilibrium decreased with increasing concentration. In the case of adsorption to hematite, this observation can be explained by the specific adsorption mechanisms. The adsorption of aqueous organic acid anions to hydrous metal oxides often involves a two-step process with rapid formation of an outer sphere complex followed by slower ligand exchange reaction with the elimination of H_2O molecules.[42,48] Increasing the

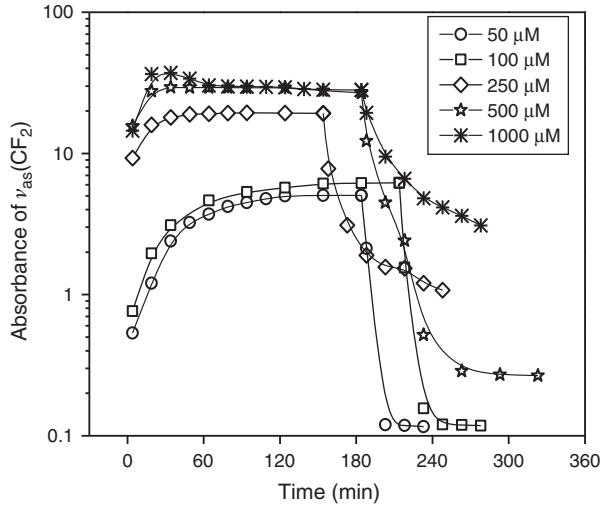

Fig. 10. Adsorption–desorption kinetics of perfluorooctanoic acid (PFOA) on hematite as represented by the IR absorbance of the $\nu_{as}(CF_2)$ band at pH 3.0 as a function of PFOA concentration.

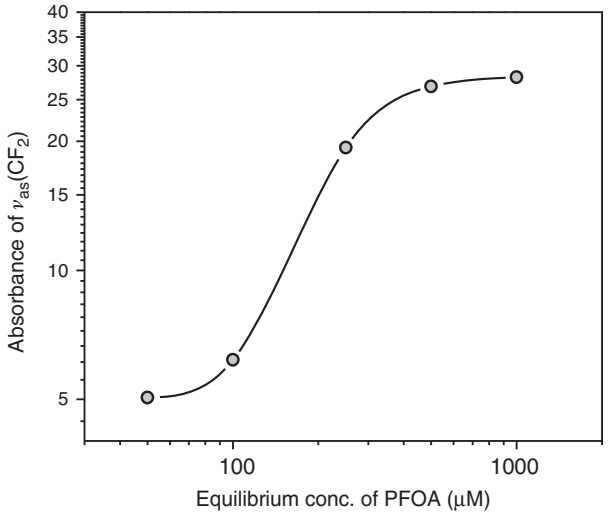

Fig. 11. Adsorption isotherm of perfluorooctanoic acid (PFOA) on hematite at pH 3.0 in 10 mM NaCl solution as represented by the IR absorbance of the $\nu_{as}(CF_2)$ band (critical micelle concentration of PFOA = 8.7–9.0 mM).

concentration of protonated reactant surface hydroxy groups ($\equiv Fe–OH_2^+$) evidently increases the reaction rate of ligand exchange, resulting in an accelerated second step for high PFOA aqueous concentration. It is noteworthy, however, that Qu et al.[48] reported similar variation in adsorption kinetics of PFOA onto powdered activated carbon in response to changing initial PFOA aqueous concentration, which presumably did not involve an inner-sphere metal complexation mechanism.

A small decrease in adsorption was observed at early reaction times for a concentration of 1000 μM PFOA (Fig. 10). This decrease is likely attributable to a surfactant-induced hematite dispersion effect whereby PFOA at high concentration formed complete bilayers on the hematite surface, reversing the charge on the Fe oxide particles, which resulted in partial displacement of the hematite film as a result of shear forces associated with fluid flow. Desorption is relatively rapid at all concentrations. When PFOA-free electrolyte solution (i.e. 10 mM NaCl) was introduced to the flow through cell, the adsorbate mass decreased quickly, and only a small sorbate mass remained after 60 min (Fig. 10).

Adsorption isotherm

The results from the PFOA adsorption experiment at pH 3.0 are depicted in the form of an adsorption isotherm in Fig. 11 using the equilibrium absorbance of the $\nu_{as}(CF_2)$ band at 1208 cm^{-1} as a measure of surface excess. The spectra are very similar across the concentration range from 50–1000 μM, indicating that the dominant adsorption mechanisms are largely independent of surface loading. The log–log scale isotherm exhibits characteristic features of ionic surfactant adsorption to charged mineral surfaces, as reported previously in the literature.[29,51] The isotherm contains several distinct regions : a low surface excess region (<100 μM), where the adsorption is dominated by covalent chemical bonding and electrostatic forces; an intermediate region with very steep slope (from 100 to ~250 μM) where lateral surfactant–surfactant hydrophobic interactions are postulated to predominate resulting in the formation of hemimicelle-like monolayer clusters on the hematite surface; and a plateau region at concentrations ≥500 μM where the surface is occupied by surfactant bilayers.

Conclusions

The adsorption mechanisms, kinetics and isotherms of PFOA and PFOS from aqueous solution to the hematite surface were examined using in situ flow through ATR-FTIR spectroscopy. To our knowledge, this is the first spectroscopic study of PFC adsorption to environmental surfaces. Our results suggest that adsorption of both PFCs to the hydrophilic hematite surface exhibits strong pH-dependence. The data also reveal different sorption mechanisms controlling the adsorption of PFOA and PFOS to hematite. In addition to electrostatic interactions, PFOA forms inner-sphere complexes at Fe metal centres, and such direct covalent bond formation may also contribute sorption energetics at low pH, whereas PFOS forms only outer-sphere complexes at the mineral surface. The kinetics of the adsorption of PFCs to hematite was generally rapid, reaching equilibrium within a few hours. Both solution pH and surface loading had profound effects on the adsorption kinetics. Faster adsorption was observed at low pH and high surface loading.

Acknowledgements

Research support was provided by the Binational Agricultural Research and Development (BARD) fund, Grant # IS-3822-06, the Water Research Foundation (Award #4269) and the University of Arizona Water Sustainability Program. The comments and views detailed herein may not be necessarily reflecting the views of the Water Research Foundation, its officers, directors, affiliates or agents. Analyses in the ALEC were supported by NSF grant CBET-0722579.

References

[1] K. Prevedouros, L. T. Cousins, R. C. Buck, S. H. Korzeniowski, Sources, fate and transport of perfluorocarboxylates. *Environ. Sci. Technol.* **2006**, *40*, 32. doi:10.1021/ES0512475

[2] C. D. Vecitis, Y. J. Wang, J. Cheng, H. Park, B. T. Mader, M. R. Hoffmann, Sonochemical degradation of perfluorooctanesulfonate in aqueous film-forming foams. *Environ. Sci. Technol.* **2010**, *44*, 432. doi:10.1021/ES902444R

[3] C. A. Moody, J. A. Field, Determination of perfluorocarboxylates in groundwater impacted by fire-fighting activity. *Environ. Sci. Technol.* **1999**, *33*, 2800. doi:10.1021/ES981355+

[4] H. P. H. Arp, C. Niederer, K. U. Goss, Predicting the partitioning behavior of various highly fluorinated compounds. *Environ. Sci. Technol.* **2006**, *40*, 7298. doi:10.1021/ES060744Y

[5] E. Kissa, *Fluorinated surfactants: Synthesis, properties, and applications* **1994** (Marcel Dekker: New York).

[6] USEPA **2002**. Revised draft hazard assessment of perfluorooctanoic acid and its salts. Available at www.ewg.org/files/EPA_PFOA_110402.pdf [Verified 4 April 2012].

[7] Q. Yuan, R. Ravikrishna, K. T. Valsaraj, Reusable adsorbents for dilute solutionseparation.5: photodegradation of organic compounds on surfactant-modified titania. *Separ. Purif. Technol.* **2001**, *24*, 309. doi:10.1016/S1383-5866(01)00136-8

[8] C. A. Moody, G. N. Hebert, S. H. Strauss, J. A. Field, Occurrence and persistence of perfluorooctanesulfonate and other perfluorinated surfactants in groundwater at a fire-training area at Wurtsmith Air Force Base, Michigan, USA. *J. Environ. Monit.* **2003**, *5*, 341. doi:10.1039/B212497A

[9] G. L. Kennedy, J. L. Butenhoff, G. W. Olsen, J. C. O'Connor, A. M. Seacat, R. G. Perkins, L. B. Biegel, S. R. Murphy, D. G. Farrar, The toxicology of perfluorooctanoate. *Crit. Rev. Toxicol.* **2004**, *34*, 351. doi:10.1080/10408440490464705

[10] C. Lau, K. Anitole, C. Hodes, D. Lai, A. Pfahles-Hutchens, J. Seed, Perfluoroalkyl acids: a review of monitoring and toxicological findings. *Toxicol. Sci.* **2007**, *99*, 366. doi:10.1093/TOXSCI/KFM128

[11] M. Murakami, C. Morita, T. Morimoto, H. Takada, Source analysis of perfluorocarboxylates in Tokyo Bay during dry weather and wet weather using sewage marker. *Environ. Chem.* **2011**, *8*, 355.

[12] D. Skutlarek, M. Exner, H. Farber, Perfluorinated surfactants in surface and drinking water. *Environ. Sci. Pollut. Res.* **2006**, *13*, 299. doi:10.1065/ESPR2006.07.326

[13] M. Murakami, K. Kuroda, N. Sato, T. Fukushi, S. Takizawa, H. Takada, Groundwater Pollution by Perfluorinated Surfactants in Tokyo. *Environ. Sci. Technol.* **2009**, *43*, 3480. doi:10.1021/ES803556W

[14] G. B. Post, J. B. Louis, K. R. Cooper, B. J. Boros-Russo, R. L. Lippincott, Occurrence and potential significance of perfluorooctanoic acid (PFOA) detected in New Jersey public drinking water systems. *Environ. Sci. Technol.* **2009**, *43*, 4547. doi:10.1021/ES900301S

[15] O. Quiñones, S. A. Snyder, Occurrence of perfluoroalkyl carboxylates and sulfonates in drinking water utilities and related waters from the United States. *Environ. Sci. Technol.* **2009**, *43*, 9089. doi:10.1021/ES9024707

[16] N. Yamashita, K. Kannan, S. Taniyasu, Y. Horii, T. Okazawa, G. Petrick, T. Gamo, Analysis of perfluorinated acids at parts-per-quadrillion levels in seawater using liquid chromatography-tandem mass spectrometry. *Environ. Sci. Technol.* **2004**, *38*, 5522. doi:10.1021/ES0492541

[17] M. Sáez, P. de Voogt, J. R. Parsons, Persistence of perfluoroalkylated substances in closed bottle tests with municipal sewage sludge. *Environ. Sci. Pollut. Res.* **2008**, *15*, 472. doi:10.1007/S11356-008-0020-5

[18] M. H. Plumlee, J. Larabee, M. Reinhard, Perfluorochemicals in water reuse. *Chemosphere* **2008**, *72*, 1541. doi:10.1016/J.CHEMOSPHERE.2008.04.057

[19] S. Rayne, K. Forest, Perfluoroalkyl sulfonic and carboxylic acids: a critical review of physicochemical properties, levels and patterns in waters and wastewaters, and treatment methods. *J. Environ. Sci. Health Part A* **2009**, *44*, 1145. doi:10.1080/10934520903139811

[20] R. Zhang, P. Somasundaran, Advances in adsorption of surfactants and their mixtures at solid/solution interfaces. *Adv. Colloid Interface Sci.* **2006**, *123–126*, 213. doi:10.1016/J.CIS.2006.07.004

[21] C. P. Higgins, R. G. Luthy, Sorption of perfluorinated surfactants on sediments. *Environ. Sci. Technol.* **2006**, *40*, 7251. doi:10.1021/ES061000N

[22] R. L. Johnson, A. J. Anschutz, J. M. Smolen, M. F. Simcik, R. L. Penn, The adsorption of perfluorooctane sulfonate onto sand, clay, and iron oxide surfaces. *J. Chem. Eng. Data* **2007**, *52*, 1165. doi:10.1021/JE060285G

[23] V. Ochoa-Herrera, R. Sierra-Alvarez, Removal of perfluorinated surfactants by sorption onto granular activated carbon, zeolite and sludge. *Chemosphere* **2008**, *72*, 1588. doi:10.1016/J.CHEMOSPHERE.2008.04.029

[24] C. You, C. Jia, G. Pan, Effect of salinity and sediment characteristics on the sorption and desorption of perfluorooctane sulfonate at sediment-water interface. *Environ. Pollut.* **2010**, *158*, 1343. doi:10.1016/J.ENVPOL.2010.01.009

[25] C. Y. Tang, Q. S. Fu, D. Gao, C. S. Criddle, J. O. Leckie, Effect of solution chemistry on the adsorption of perfluorooctane sulfonate onto mineral surfaces. *Water Res.* **2010**, *44*, 2654. doi:10.1016/J.WATRES.2010.01.038

[26] R. Xing, S. E. Rankin, Three-stage multilayer formation kinetics during adsorption of an anionic fluorinated surfactant onto germanium. 1. Concentration effect. *J. Phys. Chem. B* **2006**, *110*, 295. doi:10.1021/JP0549069

[27] S. J. Parikh, B. J. Lafferty, D. L. Sparks, An ATR-FTIR spectroscopic approach for measuring rapid kinetics at the mineral/water interface. *J. Colloid Interface Sci.* **2008**, *320*, 177. doi:10.1016/J.JCIS.2007.12.017

[28] X. D. Gao, D. W. Metge, C. Ray, R. W. Harvey, J. Chorover, Surface complexation of carboxylate adheres *Cryptosporidium parvum* öocysts to the hematite-water interface. *Environ. Sci. Technol.* **2009**, *43*, 7423. doi:10.1021/ES901346Z

[29] X. D. Gao, J. Chorover, Infrared spectroscopic study of sodium dodecylsulfate (SDS) adsorption to hematite nano-particles in aqueous systems. *J. Colloid Interface Sci.* **2010**, *348*, 167. doi:10.1016/J.JCIS.2010.04.011

[30] S. J. Hug, In situ Fourier transform infrared measurements of sulfate adsorption on hematite in aqueous solutions. *J. Colloid Interface Sci.* **1997**, *188*, 415. doi:10.1006/JCIS.1996.4755

[31] S. Goldberg, C. T. Johnston, Mechanisms of arsenic adsorption on amorphous oxides evaluated using macroscopic measurements, vibrational spectroscopy, and surface complexation modeling. *J. Colloid Interface Sci.* **2001**, *234*, 204. doi:10.1006/JCIS.2000.7295

[32] Y. S. Hwang, J. Liu, J. J. Lenhart, C. M. Hadad, Surface complexes of phthalic acid at the hematite/water interface. *J. Colloid Interface Sci.* **2007**, *307*, 124. doi:10.1016/J.JCIS.2006.11.020

[33] A. Omoike, J. Chorover, Adsorption to goethite of extracellular polymeric substances from *Bacillus subtilis*. *Geochim. Cosmochim. Acta* **2006**, *70*, 827. doi:10.1016/J.GCA.2005.10.012

[34] K. D. Dobson, A. D. Roddick-Lanzilotta, A. J. McQuillan, An in situ infrared spectroscopic investigation of adsorption of sodium dodecylsulfate and of cetyltrimethylammonium bromide surfactants to TiO_2, ZrO_2, Al_2O_3, and Ta_2O_5 particle films from aqueous solutions. *Vib. Spectrosc.* **2000**, *24*, 287. doi:10.1016/S0924-2031(00)00096-5

[35] H. Y. Li, C. P. Tripp, Use of infrared bands of the surfactant headgroup to identify mixed surfactant structures adsorbed on Titania. *J. Phys. Chem. B* **2004**, *108*, 18318. doi:10.1021/JP046741U

[36] U. Schwertmann, R. M. Cornell, *Iron Oxides in the Laboratory: Preparation and Characterization* **1991** (Wiley-VCH: Weinheim, Germany).

[37] C. A. Alves, M. D. Porter, Atomic force microscopic characterization of fluorinated alkanethiolate monolayer at gold and correlations electrochemical and infrared reflection spectroscopic structural descriptions. *Langmuir* **1993**, *9*, 3507. doi:10.1021/LA00036A027

[38] T. J. Lenk, V. M. Hallmark, C. L. Hoffmann, J. F. Rabolt, D. G. Castner, C. Erdelen, H. Ringsdorf, Structural investigation of molecular organization in self-assembled monolayers of a semifluorinated amidethiol. *Langmuir* **1994**, *10*, 4610. doi:10.1021/LA00024A037

[39] J. L. López-Fontán, F. Sarmiento, P. C. Schulz, The aggregation of sodium perfluorooctanoate in water. *Colloid Polym. Sci.* **2005**, *283*, 862. doi:10.1007/S00396-004-1228-7

[40] N. O. Brace, Long chain alkanoic and alkenoic acids with perfluoroalkyl terminal segments. *J. Org. Chem.* **1962**, *27*, 4491. doi:10.1021/JO01059A090

[41] J. Y. Ha, T. H. Yoon, Y. G. Wang, C. B. Musgrave, G. E. Brown, Adsorption of organic matter at mineral/water interfaces: 7. ATR-FTIR and quantum chemical study of lactate interactions with

hematite nanoparticles. *Langmuir* **2008**, *24*, 6683. doi:10.1021/LA800122V

[42] T. H. Yoon, S. B. Johnson, C. B. Musgrave, G. E. Brown, Adsorption of organic matter at mineral/water interfaces: I. ATR-FTIR spectroscopic and quantum chemical study of oxalate adsorbed at boehmite/water and corundum/water interfaces. *Geochim. Cosmochim. Acta* **2004**, *68*, 4505. doi:10.1016/J.GCA.2004.04.025

[43] D. L. Sparks, Sorption, in *Encyclopedia of Soils in the Environment* (Ed. D. Hillel) **2004**, pp. 532 (Academic Press).

[44] K. Nakamoto, *Infrared and Raman Spectra of Inorganic and Coordination Compounds* **1986** (Wiley: New York).

[45] R. Atkin, V. S. J. Craig, S. Biggs, Adsorption kinetics and structural arrangements of cationic surfactants on silica surfaces. *Langmuir* **2000**, *16*, 9374. doi:10.1021/LA0001272

[46] D. J. Neivandt, M. L. Gee, C. P. Tripp, M. L. Hair, Coadsorption of poly(styrenesulfonate) and cetyltrimethylammonium bromide on silica investigated by attenuated total reflection techniques. *Langmuir* **1997**, *13*, 2519. doi:10.1021/LA962047X

[47] Z. Wang, C. C. Ainsworth, D. M. Friedrich, P. L. Gassman, A. G. Joly, Kinetics and mechanism of surface reaction of salicylate on alumina in colloidal aqueous suspension. *Geochim. Cosmochim. Acta* **2000**, *64*, 1159. doi:10.1016/S0016-7037(99)00360-9

[48] Y. Qu, C. J. Zhang, F. Li, X. W. Bo, G. F. Liu, Q. Zhou, Equilibrium and kinetics study on the adsorption of perfluorooctanoic acid from aqueous solution onto powdered activated carbon. *J. Hazard. Mater.* **2009**, *169*, 146. doi:10.1016/J.JHAZMAT.2009.03.063

[49] Q. Yu, R. Q. Zhang, S. B. Deng, J. Huang, G. Yu, Sorption of perfluorooctane sulfonate and perfluorooctanoate on activated carbons and resin: kinetic and isotherm study. *Water Res.* **2009**, *43*, 1150. doi:10.1016/J.WATRES.2008.12.001

[50] J. Chorover, M. L. Brusseau, Kinetics of sorption-desorption, in *Kinetics of Water-Rock Interaction* (Eds S. L. Brantley, J. D. Kubicki, A. F. White) **2008**, pp. 109–149 (Springer: New York).

[51] M. R. Bohmer, L. K. Koopal, Adsorption of ionic surfactants on variable-charge surfaces. 1. Charge effects and structure of the adsorbed layer. *Langmuir* **1992**, *8*, 2649. doi:10.1021/LA00047A014